Phase transitions in praseodymium up to 23 GPa: An x-ray powder diffraction study

S. R. Evans, I. Loa, L. F. Lundegaard, and M. I. McMahon
SUPA, School of Physics and Astronomy and Centre for Science at Extreme Conditions, The University of Edinburgh, Mayfield Road, Edinburgh EH9 3JZ, United Kingdom

(Received 26 April 2008; revised manuscript received 11 August 2009; published 5 October 2009)

The lanthanide metal Pr has been studied by x-ray powder diffraction from 5 to 23 GPa with the aim of resolving the long-standing disagreements about the identity of the high-pressure phases, transitions, and structures of this element. We find that the distorted-fcc (d-fcc) phase observed above 7.4 GPa has the rhombohedral *hR*24 structure reported previously by Hamaya *et al.* and can definitely rule out the monoclinic structure proposed by other authors. At 13.7 GPa, the d-fcc phase starts to transform to another phase, Pr-VII, the structure of which is body-centered orthorhombic or a very slight distortion thereof. Pr-VII transforms to the α-uranium phase at 20.5(5) GPa. In addition to identifying the phase transitions and structures, we have also resolved many of the disagreements between previous diffraction studies and show that almost all previous work is in agreement with the present study. The likely existence of the Pr-VII phase in a second lanthanide, Nd, suggests that it might be an additional member of the sequence of phases observed across the lanthanide elements.

DOI: 10.1103/PhysRevB.80.134105 PACS number(s): 61.50.Ks, 62.50.−p

I. INTRODUCTION

The trivalent lanthanide elements exhibit a series of phases with close-packed crystal structures—fcc → double-hcp (dhcp) → Sm type → hcp—as a function of increasing 4*f* occupancy.[1] The same series of phases, but in reverse order, can be accessed within individual lanthanides through the application of pressure.[2] Further compression of the fcc phase leads to further phase transitions not found at ambient pressure—first to the so-called distorted-fcc (d-fcc) phase and then to one or more "collapsed" phases in which the 4*f* electrons are thought to become itinerant and to participate in the bonding. On compression, therefore, the full phase transition sequence is hcp → Sm type → dhcp → fcc → d-fcc → collapsed.

Pr is the lowest-*Z* member of the lanthanides in which the fcc → d-fcc → collapsed sequence of transitions is observed, with transition pressures of approximately 7 and 20 GPa.[2] As a consequence of the low transition pressures (compared to those found in the higher-*Z* lanthanides), the structures of the d-fcc and collapsed phases of Pr have attracted considerable attention, and the results of these numerous studies have subsequently been applied both to other members of the lanthanide series and also to some actinides.[2,3]

However, within the large body of resulting work on Pr, there is a surprising amount of disagreement as to the exact sequence of transitions and to the structure of the d-fcc phase. The first determination of this structure was made by Mao *et al.*[4] using monochromatic film-based techniques. They reported that diffraction peaks from the d-fcc phase could be indexed using an orthorhombic distortion of the fcc phase, with 16 atoms per unit cell (denoted *oP*16 in Pearson notation[5,6]). The relationship of this structure to the fcc structure is $\vec{a} \approx \vec{a}_{\mathrm{fcc}} + \vec{b}_{\mathrm{fcc}}$, $\vec{b} \approx -\vec{a}_{\mathrm{fcc}} + \vec{b}_{\mathrm{fcc}}$, and $\vec{c} \approx 2\vec{c}_{\mathrm{fcc}}$. In the same paper the authors identified the collapsed phase of Pr as having a distorted-hcp (d-hcp) structure with a volume change ($\Delta V / V_{trans}$) of 19% at the d-fcc → d-hcp transition. However, using the same data, Smith and Akella later correctly identified the collapsed phase as having the orthorhombic α-uranium (α-U) structure with four atoms per cell (*oC*4),[7] and this was subsequently confirmed in the energy-dispersive diffraction study of Grosshans *et al.*[8] The revised value for the volume change at the d-fcc → α-U transition was ~9.5%.[7,8] Smith and Akella also reinterpreted the d-fcc diffraction data of Mao *et al.*[4] and tentatively suggested the d-fcc phase as having the "missing" triple hexagonal close-packed structure.[9]

The next experimental determination of the d-fcc structure was made by Grosshans *et al.*,[10] who, again using energy-dispersive powder diffraction techniques, reported that all the observed diffraction peaks could be indexed on a hexagonal unit cell with $\vec{a} \approx -\frac{1}{2}\vec{a}_{\mathrm{fcc}} + \frac{1}{2}\vec{b}_{\mathrm{fcc}}$ and $\vec{c} \approx 2(\vec{a}_{\mathrm{fcc}} + \vec{b}_{\mathrm{fcc}} + \vec{c}_{\mathrm{fcc}})$ [see Fig. 1(a)] with six atoms per cell (*hP*6) and that the fcc → d-fcc transition therefore arose from a periodic distortion of the hexagonal close-packed layers as the result of a soft *L*-point zone-boundary phonon at $\frac{2\pi}{a_{\mathrm{fcc}}}(\frac{1}{2}, \frac{1}{2}, \frac{1}{2})$. The space group of this structure was reported as $P3_121$ or $P3_221$.[10,11] The d-fcc phases of Y and La were reported as having the same *hP*6 structure,[11] and the same structure was subsequently found in Nd, Sm, Gd, Tb, Dy,[12] and Pm.[13]

The d-fcc phase of Pr was one of the first high-pressure phases to be studied by the new angle-dispersive diffraction techniques pioneered in Japan in the early 1990s.[14] The greatly superior resolution and sensitivity afforded by the use of monochromatic synchrotron radiation and an image-plate area detector enabled Hamaya *et al.*[15] to identify a large number of additional weak peaks in the diffraction patterns from the d-fcc phase, which could all be accounted for by a rhombohedral structure, space group $R\bar{3}m$ or *R*32, with 24 atoms in the equivalent hexagonal unit cell (*hR*24). The relationship of the hexagonal setting of this structure to fcc is $\vec{a} \approx -\vec{a}_{\mathrm{fcc}} + \vec{b}_{\mathrm{fcc}}$ and $\vec{c} \approx 2(\vec{a}_{\mathrm{fcc}} + \vec{b}_{\mathrm{fcc}} + \vec{c}_{\mathrm{fcc}})$ and it is thus a $2a \times 2a \times c$ superstructure of the *hP*6 structure, as illustrated in Fig. 1(b). The transition was reported to arise from the softening of the TA phonon mode at the *L* point of the Brillouin zone. The same study reported the first Rietveld refinement

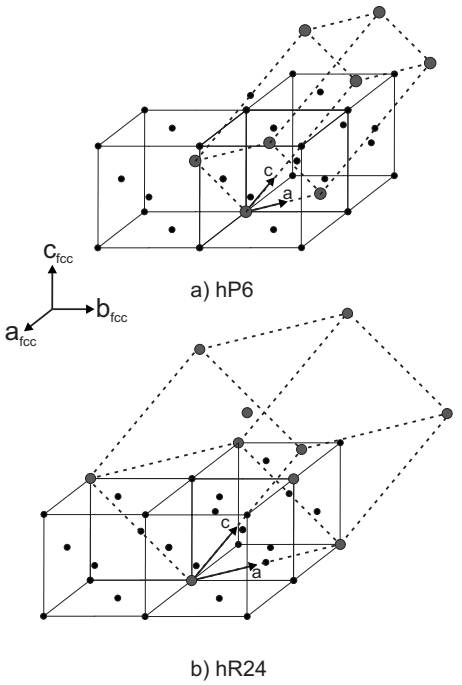

FIG. 1. The (a) *hP*6 and (b) *hR*24 structures reported for the d-fcc phase of Pr (Refs. 10 and 15). Both structures are drawn relative to the fcc structure, three unit cells of which are shown. The lattice points of the *hP*6 and *hR*24 structures are shown shaded in gray.

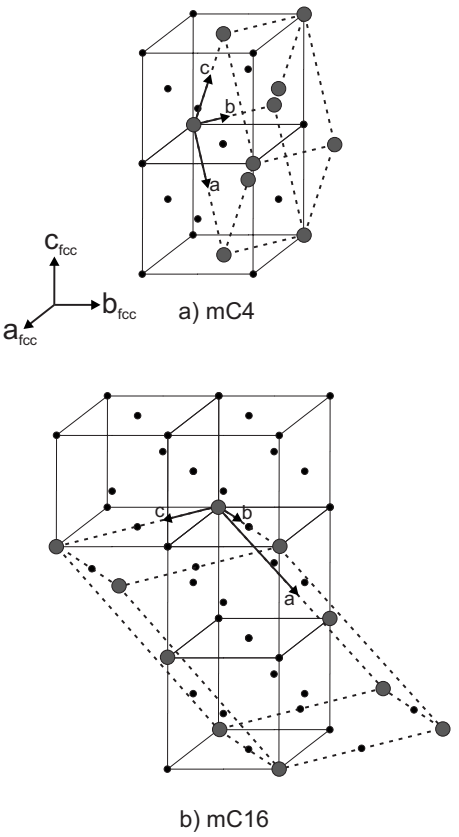

FIG. 2. The (a) *mC*4 and (b) *mC*16 structures reported for the d-fcc phase of Pr (Ref. 18 and 22). Both structures are drawn relative to the fcc structure, several unit cells of which are shown. The lattice points of the *mC*4 and *mC*16 structures are shown shaded in gray.

of the *hR*24 structure at 13.8 GPa, although the effects of texture within the sample resulted in a number of significant misfits. A further Rietveld refinement, which included a correction for preferred orientation, gave an excellent fit.[16] Interestingly, Hamaya *et al.*[15] reported that they first observed the α-U phase at about 15 GPa, significantly lower than ~20 GPa reported by Mao *et al.* and Grosshans *et al.*[4,8]

Soon after the study by Hamaya *et al.* the fcc→d-fcc transition was considered by Porsch and Holzapfel[17] on symmetry grounds, and they concluded that only one orthorhombic structure, with space group *Cmmm* and eight atoms per unit cell, was compatible both with a second-order fcc →d-fcc phase transition and the reported x-ray diffraction patterns. The relationship of this structure to that of fcc is $\vec{a} \approx 2\vec{a}_{\mathrm{fcc}}$, $\vec{b} \approx \vec{b}_{\mathrm{fcc}} + \vec{c}_{\mathrm{fcc}}$, and $\vec{c} \approx -\frac{1}{2}\vec{b}_{\mathrm{fcc}} + \frac{1}{2}\vec{c}_{\mathrm{fcc}}$. However, the authors also reported three other structures—orthorhombic with space group *Cmma*, rhombohedral with space group $R\bar{3}m$ (*hR*24), and triclinic with space group $P\bar{1}$—as possible candidates for the d-fcc phase if the fcc→d-fcc transition was first order. Subsequent Rietveld refinements using the *Cmmm*, *Cmma*, and $R\bar{3}m$ structures showed that the latter gave a significantly better fit to a diffraction profile collected at 13.8 GPa.[16]

Although the *hR*24 structure provided an excellent fit to diffraction profiles of the d-fcc phase, an unpublished high-resolution diffraction study conducted by Syassen *et al.*[18] reported that a different monoclinic structure, with space group $C2/m$ (*mC*4), also provided a good fit to the same phase above 13 GPa. The relationship of this structure to the fcc structure is $\vec{a} \approx \frac{1}{2}\vec{a}_{\mathrm{fcc}} + \frac{1}{2}\vec{b}_{\mathrm{fcc}} - \vec{c}_{\mathrm{fcc}}$, $\vec{b} \approx -\frac{1}{2}\vec{a}_{\mathrm{fcc}} + \frac{1}{2}\vec{b}_{\mathrm{fcc}}$, and $\vec{c} \approx \frac{1}{2}\vec{a}_{\mathrm{fcc}} + \frac{1}{2}\vec{b}_{\mathrm{fcc}} + \vec{c}_{\mathrm{fcc}}$ and this is illustrated in Fig. 2(a). This structure, with four atoms in the unit cell, is a subgroup of the fcc structure and had been observed previously in Ce at high pressures.[19] But although Rietveld analysis of a profile collected at 15 GPa yielded good agreement between observed and calculated profiles, close analysis of the observed and calculated diffraction profiles reveals a number of weak diffraction peaks not accounted for by the *mC*4 structure.

Shortly after this study Chesnut and Vohra[20] reported that they observed *both* the *hR*24 and *mC*4 structures in Pr over the pressure range of 7–21 GPa, with the *hR*24 structure being stable only up to 10 GPa, in disagreement with Hamaya *et al.*,[15] and the *mC*4 structure being stable from 10 GPa up to the transition to the α-U phase at 20 GPa. The calculated volume change at the *mC*4→α-U transition was 16.7% ($\Delta V/V_{trans}$).[20]

In 2003, Baer *et al.*[21] made a detailed study of the high-pressure high-temperature Pr phase diagram using a combination of energy- and angle-dispersive diffraction techniques. In addition to identifying a new high-temperature phase (which they denoted Pr-VI) between the d-fcc and α-U phases, the authors noted that they had considerable difficulty in fitting diffraction patterns collected near the d-fcc →α-U phase boundary using the *hR*24 structure. However, the authors ruled out the existence of the *mC*4 structure, noting that it led to a significant increase in the atomic vol-

ume for this phase and an unphysical increase in volume at the d-fcc $\rightarrow \alpha$-U transition.

A possible reason for the poor fit obtained with the *hR*24 structure at higher pressures was given by Dmitriev *et al.* as a result of a detailed angle-dispersive x-ray diffraction study.[22] In agreement with Chesnut and Vohra[20] and Baer *et al.*,[21] they reported that the *hR*24 structure did not give a good fit to diffraction profiles collected above 12 GPa and proposed that above this pressure there was a new phase with a monoclinic structure, space group $C2/m$, with 16 atoms per unit cell (this *mC*16 monoclinic structure is therefore different to the *mC*4 structure proposed by Syassen *et al.* and also observed by Chesnut and Vohra). The relationship of the *mC*16 structure to that of fcc is $\vec{a} \approx -\vec{a}_{\mathrm{fcc}} + \vec{b}_{\mathrm{fcc}} - 2\vec{c}_{\mathrm{fcc}}$, $\vec{b} \approx \vec{a}_{\mathrm{fcc}} + \vec{b}_{\mathrm{fcc}}$, and $\vec{c} \approx \vec{a}_{\mathrm{fcc}} - \vec{b}_{\mathrm{fcc}}$, and this is illustrated in Fig. 2(b).

This new monoclinic phase, which they denoted Pr-VII, was reported to be stable up to 25 GPa, the reported transition pressure to the α-U phase, which is some 5 GPa higher than that reported by previous authors. A consequence of the existence of the new *mC*16 structure above 12 GPa is that the compressibility of Pr changes at the *hR*24 $\rightarrow$ *mC*16 transition, resulting in a larger volume change at the d-fcc $\rightarrow \alpha$-U transition than if the volume of the *hR*24 structure was extrapolated to the transition pressure. However, the volume per atom quoted by Dmitriev *et al.* for the *mC*16 structure at 19.1 GPa (21.969 Å^3) is both inconsistent with that calculated from the reported lattice parameters at the same pressure (22.204 Å^3) and with that shown in Fig. 4 in Ref. 22 at the same pressure ($\sim$23 Å^3). The compressibility of Pr in this pressure range thus appears unclear.

Although the study of Dmitriev *et al.*[22] at first seemed to clarify the high-pressure behavior of Pr, further uncertainty as to the transition sequence has been added by the two most recent studies. First, in a subsequent Raman study of the d-fcc phase, Olijnyk *et al.*[23] used only the *mC*4 structure to interpret their data between 10 and 20 GPa, while in the most recent angle-dispersive x-ray diffraction study, Cunningham *et al.*[24] could not confirm the existence of the *mC*4 structure and reported that the *hR*24 structure was stable over the full pressure range of 7–19 GPa with a volume change of 9.1% at the transition to the α-U phase. Neither of these studies reported observing the *mC*16 structure.

There is also considerable uncertainty as to the identity of the contaminant peaks observed in almost all of the diffraction studies of Pr. Hamaya *et al.*[15] noted that their diffraction profiles contained six peaks not accounted for by the *hR*24 structure and that four of these could be indexed as coming from PrO having the rocksalt structure with $a = 4.9593(9)$ Å at 13.8 GPa. The other two peaks had d spacings of 2.390 and 1.690 Å at the same pressure. The same authors noted that the data of Mao *et al.*[4] contained four diffraction peaks from the same cubic PrO phase and also a single additional peak at $d = 1.690$ Å. (In fact, the table of observed d spacings given by Mao *et al.* at 14.4 GPa does not contain a peak at $d = 1.690$ Å, only one at $d = 1.698$ Å). Although Hamaya *et al.* do not comment on the identity of the two additional peaks they observe, the ratio of the peaks' d spacings is $\sqrt{2}$ and they might therefore be explained as the (200) and (220) diffraction peaks from a second cubic contaminant with $a = 4.780$ Å at 13.8 GPa.

The study of Chesnut and Vohra[20] labels two peaks in a diffraction profile obtained at 9 GPa as coming from an oxide, but it does not identify its formula. Baer *et al.*[21] noted the proclivity of Pr to oxidize rapidly if not protected by mineral oil or an inert atmosphere and also considered the effects of hydrogen within the sample. On heating above 650 K, contaminant peaks identified as coming from PrH_{2+x} resulting from a reaction of the Pr sample with the mineral oil pressure medium were observed to grow, and these remained on both temperature and pressure decrease. No such contaminants were observed if Ar was used as the pressure medium. Dmitriev *et al.*,[22] using samples loaded under both mineral oil and argon, also observed a number of weak additional contaminant peaks, which, from the extrapolated lattice parameter at ambient pressure, they assigned to cubic PrO, in agreement with Hamaya *et al.*[15] Finally, in the most recent diffraction study, Cunningham *et al.* noted that they could index the small amount of oxide in their study as coming from PrO_2 with the cubic fluorite structure.[24] There thus seems to be no clear consensus on the identity of the contaminant peaks.

It is therefore clear that despite the considerable number of diffraction studies of Pr by at least nine groups over a 30 year period, there is clearly still a great deal of uncertainty as to the structural behavior of Pr between 7 and 20 GPa. In particular (i) what is the structure of the d-fcc phase of Pr between 7 and 10–12 GPa? (ii) Is there a phase transition at 10–12 GPa to another, possibly monoclinic, phase? (iii) What is the identity of the contaminant phase(s)?

Resolving these uncertainties in Pr is important, as a detailed knowledge of the structures and transitions of the d-fcc phase is then transferable to the very similar behavior reported for other trivalent lanthanide elements.[12] To address these issues, we have therefore undertaken a detailed x-ray powder diffraction study of Pr up to 23 GPa using angle-dispersive techniques.

II. EXPERIMENTAL DETAILS

High-pressure diffraction experiments were carried out using Pr of 99.99% purity purchased from Alfa Aesar and from a distilled ingot of 99.98% purity supplied by U. Schwarz at the Max-Planck-Institut für Chemische Physik fester Stoffe in Dresden. Small pieces of Pr were cut from these larger ingots and were loaded into diamond anvil cells either under dry mineral oil or in a glovebox with a dry inert argon atmosphere. No pressure transmitting medium was used in the case of the glovebox-loaded samples, while dry mineral oil was used for samples loaded under oil. In total, 11 samples were loaded into nine different pressure cells. Gaskets made from tungsten foil of an initial thickness of 200 μm were preindented to $\sim$25 μm before sample chambers of 100 μm diameter were drilled by spark erosion. Small (5 μm diameter) ruby spheres were loaded with the samples for pressure measurement using the ruby fluorescence method,[25] with the calibration of Mao *et al.*[26]

Diffraction data were collected on stations 9.1 and 9.5HPT at the Synchrotron Radiation Source, Daresbury

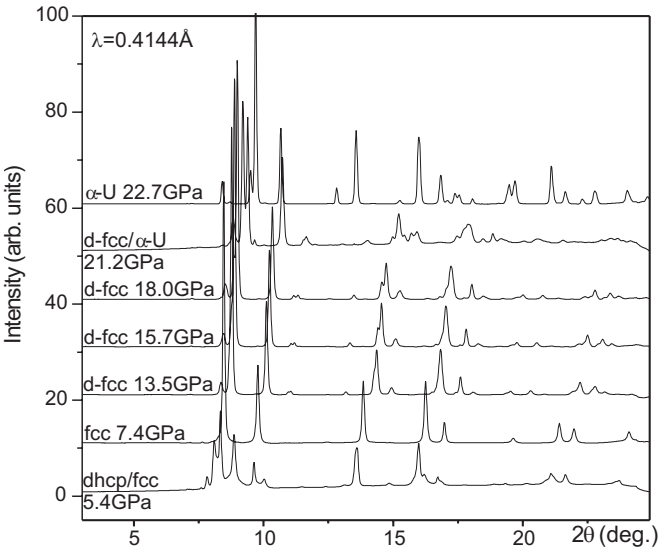

FIG. 3. Typical diffraction profiles from mixed dhcp/fcc, fcc, d-fcc, mixed d-fcc/α-U, and α-U phases of Pr collected on pressure increase from 5.4 to 22.7 GPa. The d-fcc and α-U phases first appear at 7.4(2) and 20.5(5) GPa, respectively, on pressure increase.

Laboratory. A few diffraction profiles were also collected on beamline ID09A at the European Synchrotron Radiation Facility (ESRF). The incident x-ray wavelength was ~0.4 Å in both cases. Two-dimensional (2D) diffraction images were collected on an image-plate area detector placed ~360 mm from the sample, and the resulting 2D diffraction images were integrated azimuthally using FIT2D[27] to give standard diffraction profiles. A total of 185 different diffraction profiles were collected. Structural analysis was performed using the LeBail and Rietveld fitting algorithms in JANA2000.[28]

III. RESULTS

Figure 3 shows a series of diffraction profiles collected on pressure increase from 5.4 to 22.7 GPa. Peaks from the d-fcc phase were first observed at 7.4(2) GPa on pressure increase and those from the α-U phase at 20.5(5) GPa, in agreement with the transition pressure reported previously.[4,8,12] There are also indications of changes in the diffraction pattern at ~14 GPa, similar to those reported by Dmitriev *et al.*[22] Before continuing with a detailed discussion of the behavior of Pr itself under pressure, it will be useful to first consider the hydrostaticity of the sample conditions during the experiment and then to identify and discuss the nature of the contaminant phases.

A. Hydrostaticity

As mentioned above, experiments were performed using either no pressure medium or using dry mineral oil, and the same results were obtained in each case. Only data collected from samples loaded with a pressure medium were subsequently used for analysis. Previous high-pressure studies of Pr have also used no medium,[20–23] citing the softness of Pr; mineral oil,[10,15,21,22] citing its inertness at high temperature; or argon.[21] Mineral oil is reported to be nonhydrostatic above 4–5 GPa,[29] although recent measurements on the hydrostatic pressure limits of many commonly used pressure media[30] have shown that the effects of nonhydrostaticity appear lower than previously believed. Analysis of the previous high-pressure studies of Pr shows no systematic difference in phase behavior or transition pressures resulting from the choice of pressure medium, in agreement with the behavior observed in the present study.

Any pressure gradients in the sample can be quantified from the pressure readings from the individual ruby sphere manometers within the sample chamber. No evidence of any such gradients was observed in our studies. In addition, well resolved ruby spectra were observed to the highest pressures.[25] The existence of anisotropic stress in the sample arising from nonhydrostaticity can also be determined from the x-ray diffraction profiles themselves and is evident as *hkl*-dependent shifts in diffraction peak positions.[31] Using the method of Takemura and Singh,[32] we find no measurable differential stress in the fcc phase of Pr at 7.4 GPa. Similarly, analysis of the diffraction profiles from the d-fcc, Pr-VII, and α-U phases at 12.5 (Fig. 6), 19.0 (Fig. 14), and 21.8 (Fig. 18) GPa, respectively, also shows no evidence of any differential stress resulting in *hkl*-dependent peak shifts. We conclude, therefore, that any effects of nonhydrostaticity in the present study are too small to detect.

B. Contaminant phases

Present in all our diffraction data, along with diffraction peaks from Pr, are peaks originating from contaminants. This is a well-known problem inherent in studies of this element, although, as said, the exact identity of the contaminants remains unclear. The presence of the contaminants is easily identified in both the one-dimensional integrated profiles and 2D diffraction images because of the regular fcc spacing and characteristic texture of the diffraction peaks, respectively. This is illustrated in Fig. 4 which shows an enlarged view of a diffraction profile from d-fcc Pr at 10.4 GPa. The additional contaminant peaks are indicated with arrows, and their regular spacing is consistent with two contaminants, both of which are cubic with an fcc lattice. One of these, the peaks of which are indicated with asterisks, is the cubic PrO phase identified by Hamaya *et al.*,[15] while the second phase has a slightly smaller lattice parameter. The inset of Fig. 4 shows part of the 2D diffraction image from the same pattern. It is clear that the diffraction rings from the PrO contaminant have a very spotty texture, which enables them to be identified easily.

Numerous attempts to load samples with no contamination were unsuccessful, one or both of the cubic contaminants were always observed, although with varying proportions. The pressure dependence of the lattice parameters of the two contaminants is shown in Fig. 5. At pressures below 5 GPa, the peaks from both contaminants are overlapped by peaks from the Pr and it was therefore not possible to determine the lattice parameters. Also shown in Fig. 5 are the ambient pressure lattice parameters of PrO,[33] PrO_2,[34] and PrH_2.[35] Extrapolation of our data to ambient pressure suggests that (i) both of the contaminants will have lattice pa-

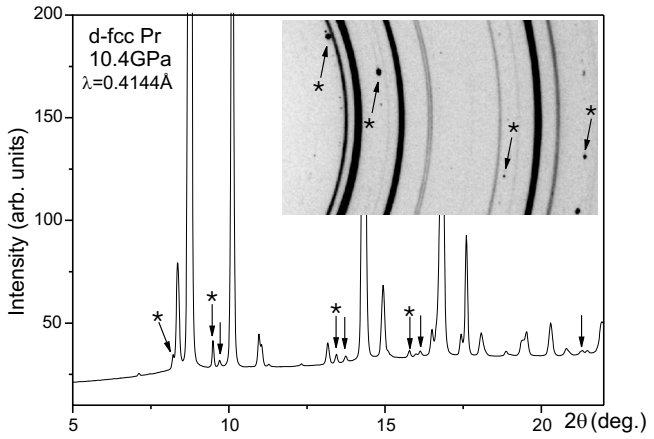

FIG. 4. Diffraction profile from the d-fcc phase of Pr at 10.4 GPa. The additional diffraction peaks are identified with arrows and come from two cubic contaminants, each with an fcc lattice. The contaminant peaks arising from the PrO contaminant identified by Hamaya *et al.* are indicated with asterisks. The inset shows part of the 2D diffraction pattern from the same sample, showing the spotty nature of the PrO diffraction rings.

rameters that are slightly larger than those one would expect if they were PrO and (ii) neither of the contaminants is PrO_2 or PrH_2. Further data below 5 GPa will be required in order to uniquely identify the contaminants from their ambient pressure lattice parameters.

C. Structure of the d-fcc phase from 7–14 GPa

The fcc→d-fcc transition was observed at 7.4(2) GPa on pressure increase, and there is evidence of further changes in the diffraction patterns at ~14 GPa. The nature of these latter changes is discussed later in this paper, and we will therefore restrict our discussion initially to the behavior of Pr between 7 and 14 GPa.

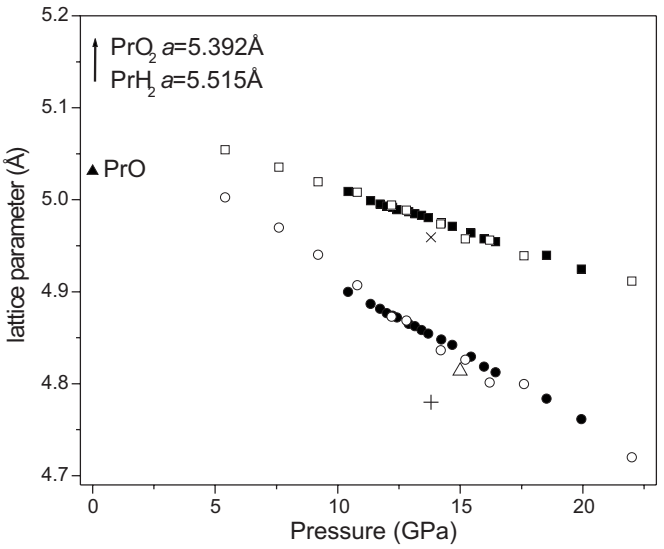

FIG. 5. Pressure dependence of the lattice parameters of the two cubic contaminant phases present in our samples. Data collected on pressure increase/decrease are shown using solid/hollow symbols. Also shown are the lattice parameter of PrO reported by Hamaya *et al.* at 13.8 GPa (×); the calculated cubic lattice parameter from the two additional unidentified peaks reported by the same authors (+); and the calculated cubic lattice parameter (△) obtained from the *d* spacing of the contaminant peak misidentified by Chesnut and Vohra (Ref. 20).

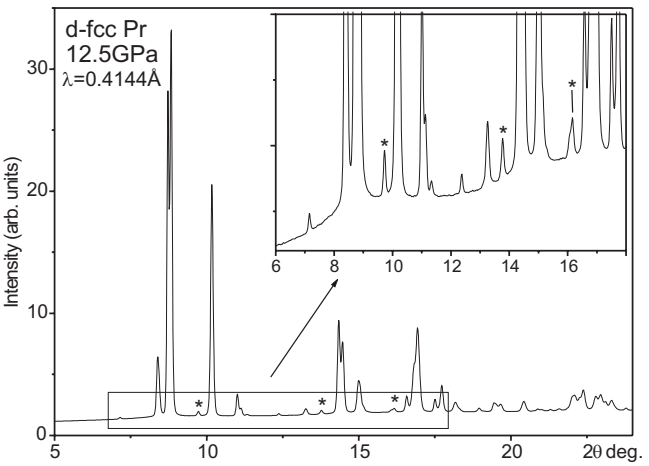

FIG. 6. High-resolution diffraction profile obtained from the d-fcc phase of Pr at 12.5 GPa. The inset shows an enlarged view of some of the very weak diffraction peaks. In this sample, diffraction peaks from only one of the cubic contaminant were present, and these are indicated with asterisks.

On pressure increase above 7.4 GPa, many of the reflections from the fcc phase split into a number of peaks, the separation of which increases with pressure, thereby aiding structure solution. A diffraction pattern from the d-fcc phase at 12.5 GPa is shown in Fig. 6 and a Rietveld fit to this profile using the *hR*24 structure of Hamaya *et al.*[15] is shown in Fig. 7. In this structure, atoms are located on the 6*c* and 18*h* sites of space group $R\bar{3}m$ at $(0,0,z_1)$ and $(x,-x,z_2)$, respectively. All the noncontaminant peaks, even the weakest (as illustrated in the inset of Fig. 7), are accounted for, and

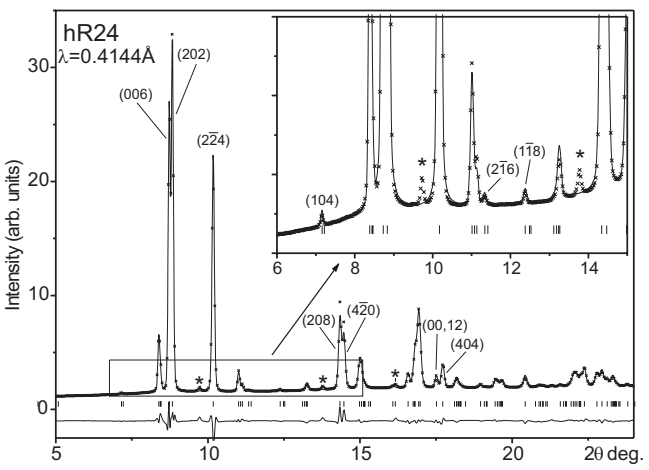

FIG. 7. Rietveld refinement of the rhombohedral *hR*24 structure to the diffraction pattern of d-fcc Pr obtained at 12.5 GPa. Indices are given for key reflections and asterisks mark the contaminant peaks. The tick marks below the profile show the calculated peak positions, and the difference between the observed and calculated profiles is shown below the tick marks. The inset shows an enlarged view of the fit to the weak reflections at low angles.

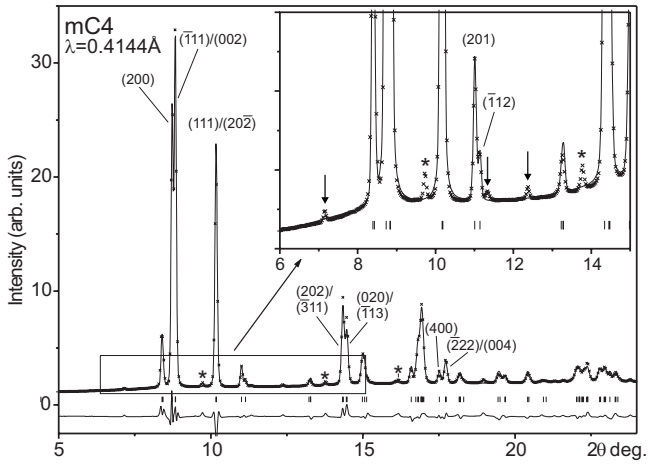

FIG. 8. Rietveld refinement of the monoclinic *mC*4 structure to the diffraction pattern of d-fcc Pr obtained at 12.5 GPa. Indices are given for key reflections and asterisks mark those reflections from the contaminants. The tick marks below the profile show the calculated peak positions, and the difference between the observed and calculated profiles is shown below the tick marks. The inset shows an enlarged view of the fit to the weak reflections at low angles, illustrating the inability of this structure to account for all the observed reflections, as marked by arrows.

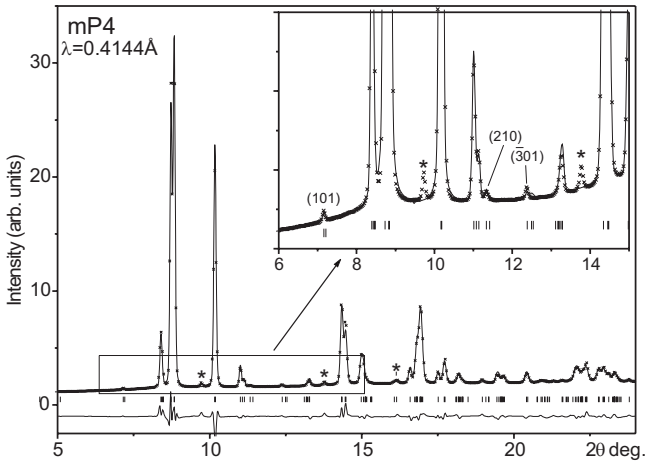

FIG. 9. Rietveld refinement of the monoclinic *mP*4 structure to the diffraction pattern of d-fcc Pr obtained at 12.5 GPa. Indices are given for key reflections and asterisks mark those reflections from the contaminants. The tick marks below the profile show the calculated peak positions, and the difference between the observed and calculated profiles is shown below the tick marks. The inset shows an enlarged view of the fit to the weak reflections at low angles, illustrating the greatly improved fit obtained by removing the C-centered symmetry.

the fit to the observed peak intensities is excellent. The refined structural parameters are $a=6.5429(1)$ Å, and $c=16.2403(4)$ Å [volume/atom=25.09(1) Å^3] with atoms at (0,0,0.2706(2)) and (0.5068(2),−0.5068(2),0.2427(2)). Analysis of Fig. 1 of Chesnut and Vohra[20] shows that these authors indexed a diffraction peak in the *hR*24 diffraction pattern as (106). This reflection is absent in space group $R\bar{3}m$ as it violates the general $-h+k+l=3n$ reflection condition. The diffraction peak is actually the (200) peak from one of the cubic contaminants discussed in Sec. III B, as can be seen from Fig. 5, which shows the calculated lattice parameter obtained from the *d* spacing of this reflection at 15 GPa.

Figure 8 shows a Rietveld fit to the same 12.5 GPa d-fcc diffraction profile using the *mC*4 structure of Syassen *et al.*[18] The refined structural parameters are $a=5.7303(2)$ Å, $b=3.2751(4)$ Å, $c=5.6597(7)$ Å, and $\beta=109.15(5)°$ [volume/atom=25.08(1) Å^3] with atoms on the 4*i* site of space group $C2/m$ at (0.2838(2),0,0.2460(4)). While the structure does provide a very good fit to the strong diffraction peaks, enlargement of the weakest peaks (inset in Fig. 8) shows that the structure cannot account for them and cannot therefore be correct. The same misfits are also evident in the data of Syassen *et al.*[18] Our refined lattice parameters for the *mC*4 structure, particularly the β angle, are notably different from those reported by Chesnut and Vohra at 15 GPa.[20] However, the reflection misidentified by them as the (106) reflection in the *hR*24 profile is also misidentified as the (20$\bar{2}$) reflection in the *mC*4 profile at 15 GPa (see Fig. 1 in Ref. 20). The (20$\bar{2}$) reflection should have a very similar *d* spacing to that of the (111) (see Fig. 8), and reindexing the reported *d* spacings accordingly gives refined lattice parameters of $a=5.619(9)$ Å, $b=3.18(1)$ Å, $c=5.56(2)$ Å, and $\beta=109.2(2)°$ [volume/atom=23.45(8) Å^3], in considerably better agreement with our own results and resulting in a denser structure.

The excellence of the fit of the *mC*4 structure to the strong peaks of the d-fcc phase in both position and intensity suggests that a small distortion of this structure might provide a better fit to the weaker peaks. Figure 9 shows a Rietveld fit to the same 12.5 GPa d-fcc profile using a monoclinic structure with space group $P2/m$, a subgroup of $C2/m$ in which the C centring is absent. The refined structural coordinates of this *mP*4 structure are $a=5.7303(3)$ Å, $b=3.2754(4)$ Å, $c=5.6590(7)$ Å, and $\beta=109.15(1)°$ [volume/atom=25.08(1) Å^3] with atoms on the 2*m* and 2*n* sites at (0.7101(5),0,0.7474(13)) and $(0.2219(5),\frac{1}{2},0.7580(10))$, respectively. The fit is excellent, with all the observed diffraction peaks accounted for.

Thus, at 12.5 GPa, diffraction patterns from the d-fcc phase of Pr are very well accounted for by both the *hR*24 and *mP*4 structures, while the *mC*4 structure can definitely be ruled out because of its inability to account for the weakest diffraction peaks. We note that ruling out the *mC*4 structure requires the observation of the very weak reflections marked by arrows in the inset of Fig. 8. If only the most intense Bragg reflections are observed, then ruling out the *mC*4 structure is not possible. We also note that the *hR*24, *mC*4, and *mP*4 structures all have the same density. The previous reports[20] of the *mC*4 structure having a lower density than *hR*24 arose from a misindexing of the d-fcc diffraction patterns (see above). The report of an unphysical increase in volume at the $hR24 \rightarrow mC4$ transition[21] may have resulted from the same misindexing.

Other previously proposed structures for the d-fcc phase such as *Cmmm* and *Cmma* have been ruled out previously[16] and refinements of the 12.5 GPa profile with these structures show them to give very poor fits. The question then remains

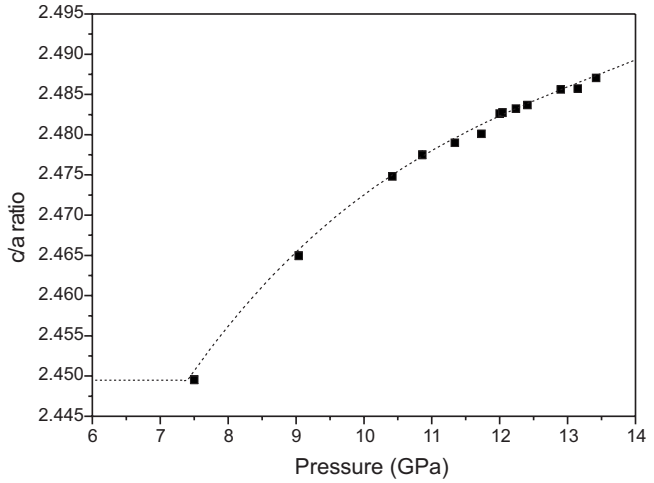

FIG. 10. The pressure dependence of the c/a ratio in the $hR24$ structure. Below 7.4 GPa, in the fcc phase, the c/a ratio takes the value $\sqrt{6}$. The data point at 7.5 GPa is from a sample that was clearly in the $hR24$ phase, as determined from the presence of non-fcc diffraction peaks. The dashed line through the data points is a guide for the eyes.

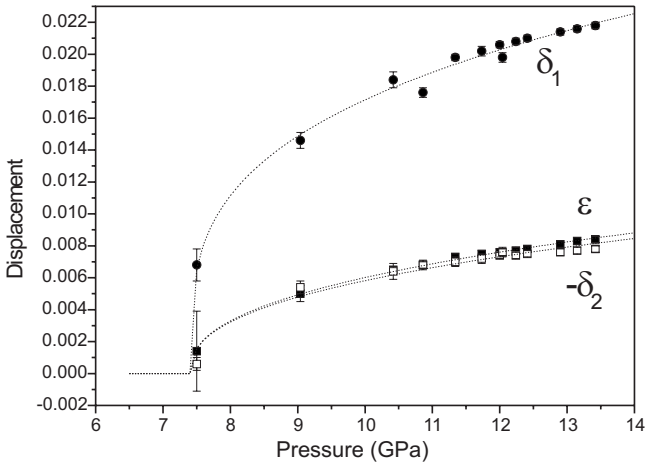

FIG. 11. The pressure dependence of the static atomic displacements ϵ, δ_1, and $-\delta_2$ in the $hR24$ structure as a function of pressure. The dashed lines correspond to least-squares fits of the data to the power law $A(P-P_c)^{\beta}$, where A and β are variable parameters and P_c is fixed at 7.4 GPa. The best fitting values of β to the pressure dependence of δ_1, ϵ, and $-\delta_2$ are 0.29(1), 0.41(1), and 0.40(1), respectively.

as to which of $hR24$ and $mP4$ is the correct structure for the d-fcc phase. $hR24$ has the higher symmetry and has only five refinable structural parameters (a, c, z_1, x, and z_2), while the $mP4$ structure has eight (a, b, c, β, x_1, z_1, x_2, and z_2). Furthermore, the lower symmetry of the monoclinic structure predicts many more reflections than the $hR24$ structure, none of which are observed, and also predicts a number of very closely spaced doublets (see inset of Fig. 9), again none of which are observed. While a definitive answer will require a single-crystal diffraction study of the d-fcc phase, there is currently no experimental evidence to favor the $mP4$ structure over the $hR24$ structure proposed by Hamaya *et al.*[15]

D. Pressure dependence of *hR*24 from 7–14 GPa

The $hR24$ structure is identical to fcc when $c/a=\sqrt{6}$ and the atoms located at $(0,0,z_1)$ and $(x,-x,z_2)$ have $z_1=\frac{1}{4}$, $x=\frac{1}{2}$, and $z_2=\frac{1}{4}$. The distortion of $hR24$ from fcc can thus be quantified by departures from these fcc-like parameters. Figure 10 shows the pressure dependence of the c/a ratio from 7 to 14 GPa. The distortion of the cubic unit cell shows no discontinuity at the fcc$\rightarrow hR24$ transition, despite this transition being first order (from symmetry arguments[17]). Following the analysis of Hamaya *et al.*,[15] the displacement of the atoms accompanying the fcc$\rightarrow hR24$ transition can be expressed by the amplitudes of the three static displacements, $\epsilon=x-\frac{1}{2}$, $\delta_1=z_1-\frac{1}{4}$, and $\delta_2=z_2-\frac{1}{4}$. The pressure dependence of ϵ, δ_1, and $-\delta_2$ is shown in Fig. 11. The results are very similar to those reported previously by Hamaya *et al.* in that (i) the distortions away from the fcc phase are continuous and (ii) that over the entire stability of the d-fcc phase, $\epsilon\approx -\delta_2\approx\frac{1}{3}\delta_1$. This relationship between the distortions arises from the inter-relations between the amplitudes of atomic displacements given by a linear combination of three equal-amplitude zone-boundary transverse acoustic phonons in the fcc structure, with wave vectors $q_1=\frac{2\pi}{a_{\mathrm{fcc}}}(\frac{1}{2},\frac{1}{2},-\frac{1}{2})$, $q_2=\frac{2\pi}{a_{\mathrm{fcc}}}(-\frac{1}{2},\frac{1}{2},\frac{1}{2})$, and $q_3=\frac{2\pi}{a_{\mathrm{fcc}}}(\frac{1}{2},-\frac{1}{2},\frac{1}{2})$.[15] Comparison of Figs. 10 and 11 shows that while there is no detectable departure from cubic symmetry at 7.5 GPa (c/a ratio$=\sqrt{6}$), the appearance of additional non-fcc reflections shows that there are already displacements of the atoms at this pressure, as is evident from the refined displacements at 7.5 GPa. This appearance of non-fcc reflections prior to any measurable distortion of the cubic lattice has been noted previously both in Pr (Ref. 18) and in a number of other lanthanide elements, but with slightly different behavior in each case.[12,18] Such behavior is consistent with the fcc$\rightarrow$d-fcc transition resulting from the softening of the TA phonon mode at the L point of the Brillouin zone,[15] which would lead initially to atomic displacements (resulting in the appearance of non-fcc reflections) followed by an elastic distortion to rhombohedral symmetry that results in a splitting of diffraction peaks.

E. Phase transition in Pr at 14 GPa

Figure 12 shows a diffraction pattern from d-fcc Pr at 10.4 GPa, and the insets show enlarged views of how the (006)/(202) and (00,12)/(404) doublets (indexed on the $hR24$ structure) evolve on pressure increase to 19.9 GPa. In the (006)/(202) doublet at $\sim 9°$, there is a gradual change in the relative intensity of the two peaks on pressure increase, such that above 16 GPa, the lower-angle (006) reflection becomes more intense than the (202). This behavior is the same as that reported by Dmitriev *et al.*[22] The (006) reflection also becomes significantly broader above 14 GPa and has the appearance of being a closely-spaced doublet before sharpening up again above 18 GPa. Syassen *et al.* also noted that above 13 GPa a triplet of reflections was resolved.[18] While the observed changes in relative intensity *might* result from pressure-induced changes in texture, a clearer illustration of what is happening can be seen in the pressure evolution of

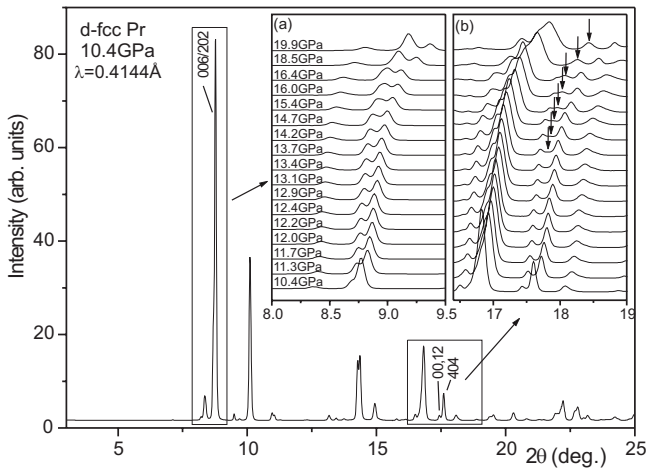

FIG. 12. The diffraction profile from d-fcc Pr at 10.4 GPa. The insets show the how (a) the (006)/(202) and (b) the (00,12)/(404) doublets (all as indexed on the *hR*24 structure) evolve on pressure increase to 19.9 GPa. The new reflection that appears between the (00,12) and (404) peaks above 13.5 GPa is indicated with an arrow in inset (b).

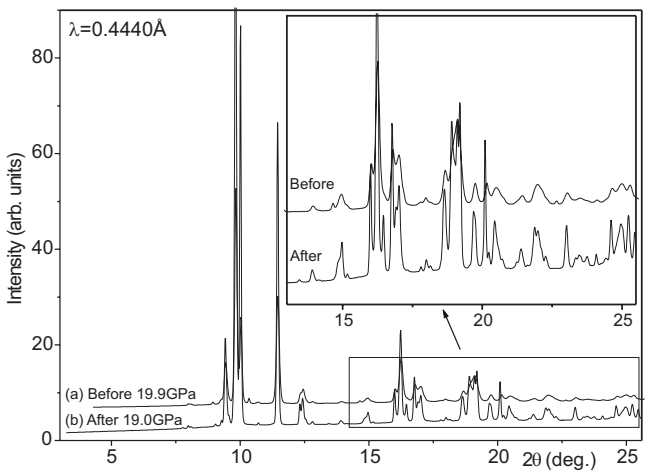

FIG. 13. Diffraction profiles from Pr-VII (a) before and (b) after annealing at 473K for 2 h. After annealing the pressure had dropped from 19.9 to 19.0 GPa. The inset shows an enlarged view of the high-angle part of the profiles, showing the dramatic sharpening of the diffraction peaks that results from annealing.

the (00,12)/(404) doublet—that is the $(2h,2k,2l)$ equivalents of the first doublet—at 17.5°. At 13.7 GPa, there is clear evidence of a new reflection appearing between the (00,12) and (404) peaks, and this new peak increases in intensity with increasing pressure. Simultaneously, the (00,12) reflection decreases in intensity and disappears completely at 19.9 GPa. The appearance of a new reflection, and the simultaneous disappearance of a reflection from the *hR*24 structure, provides definite evidence of a transition to a new phase of Pr starting at 13.7 GPa on pressure increase and being complete at 19.9 GPa. In accordance with Dmitriev *et al.*[22] we refer to this new phase as Pr-VII. Analysis of the diffraction patterns between 14 and 19 GPa suggests that there is a great deal of overlap of the reflections from the new phase with those from the *hR*24 structure, greatly complicating analysis of the new phase. And while the disappearance of the (00,12) reflection at 19.9 GPa suggests that a single-phase pattern of Pr-VII was obtained at this pressure (see insets of Fig. 12), the broadness of the diffraction peaks at this pressure again hindered analysis.

However, we found that gentle annealing of single-phase Pr-VII samples at 473K could lead to a significant sharpening of the diffraction peaks. This is illustrated in Fig. 13, which shows diffraction patterns from the same sample as in Fig. 12 before and after annealing at 473K for 2 h. After annealing the sample pressure had dropped from 19.9 to 19.0 GPa.

F. Structure of Pr from 14–20 GPa

Rietveld profile refinement of the high-resolution Pr-VII profile at 19.0 GPa using the monoclinic *mC*16 structure of Dmitriev *et al.*[22] gave a good fit, with final refined lattice parameters of $a=10.951(1)$ Å, $b=6.2012(3)$ Å, $c=6.3817(3)$ Å, and $\beta=125.71(1)°$, with atoms at (0.767(1),0,0.228(2)), (0.266(1),0,0.312(1)), and (0.002(1),0.753(2),0.235(1)). These parameters are similar to those reported by Dmitriev *et al.* at 19.1 GPa [$a=10.984(2)$ Å, $b=6.3810(2)$ Å, $c=6.275(3)$ Å, and $\beta=126.12(1)°$] with the notable difference that the relative magnitudes of the b and c lattice parameters are reversed. Attempts to fit the structure after swapping the b and c lattice parameters so that $b>c$ were unsuccessful, and the resulting Rietveld fits were very poor.

The fit to the Pr-VII profile using the best-fitting *mC*16 structure is shown in Fig. 14 and although there is close agreement between the observed and calculated profiles, it is noticeable that there is an extraordinary degree of overlap in

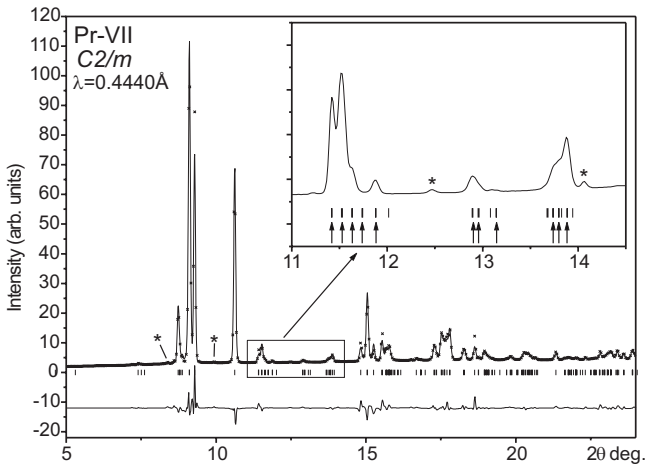

FIG. 14. Rietveld refinement of the monoclinic *mC*16 structure of Dmitriev *et al.* to the diffraction pattern of Pr-VII obtained at 19.0 GPa. The tick marks below the profile show the calculated peak positions, and the difference between the observed and calculated profiles is shown below the tick marks. Asterisks mark those reflections from the contaminants. The inset shows an enlarged view of a midangle part of the pattern. All those tick marks highlighted by arrows comprise either two or more closely-spaced or overlapped tick marks.

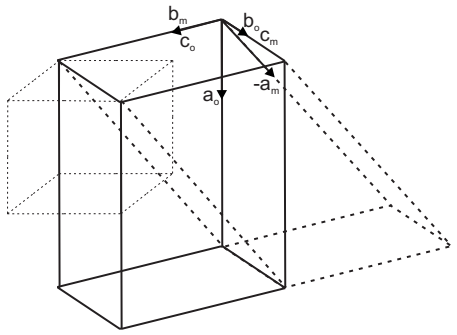

FIG. 15. The relationship between the orthorhombic *oI*16 unit cell (heavy solid lines) proposed here for Pr-VII and the monoclinic *mC*16 unit cell of Dmitriev *et al.* (heavy dashed lines). The fcc unit cell is also shown for comparison, outlined in light dashed lines.

the predicted peak positions, the majority of which are either completely overlapped or form closely-spaced doublets or multiplets—as highlighted in the inset of Fig. 14. Such a degree of overlap suggests that the structure might have a higher symmetry than monoclinic.

Initial attempts to reindex the whole Pr-VII diffraction pattern were unsuccessful, but indexing a subset of the intense peaks showed that they could be fitted extremely well with a body-centered orthorhombic unit cell with $a=4.4466(5)$ Å, $b=3.1904(3)$ Å, and $c=3.0997(4)$ Å, that is, $a \approx a_{\mathrm{fcc}}$ and $b \approx c \approx a_{\mathrm{fcc}}/\sqrt{2}$. Trial and error showed that all of the Pr-VII reflections could be accounted for by a $2\times2\times2$ supercell of this cell, that is, a body-centered orthorhombic cell with 16 atoms per unit cell (*oI*16) and $a=8.8943(13)$ Å, $b=6.3805(8)$ Å, and $c=6.2002(10)$ Å. The atom volume is 21.99(1) Å^3. We note that the relative dimensions of the Pr-VII unit cell are the same as those proposed by Mao *et al.*[4] for the d-fcc phase, although the cell proposed in that study was primitive rather than body centered. Also, the pressure in that study (14.4 GPa) and the intensity ratio of the (006)/(202) doublet (as indexed on the *hR*24 unit cell) suggest that Mao *et al.* were observing the *hR*24 structure in their study rather than Pr-VII. The relationship of the orthorhombic unit cell to the *mC*16 unit cell of Dmitriev *et al.* is shown in Fig. 15.

Analysis of the Pr-VII diffraction profile revealed that the highest-symmetry space group consistent with the observed reflections was *Ibam* and trial LeBail fits to the profile showed that this space group did indeed account for all the observed Pr-VII reflections. Transformation of the fcc structure into the *Ibam* unit cell suggested that the structure has atoms on the 8*g* and 8*j* sites at $(0,y_1,\frac{1}{4})$ and $(x,y_2,0)$, respectively, with $x \approx y_1 \approx \frac{1}{4}$ and $y_2 \approx 0$. Using these starting positions, the Pr-VII profile refined straightforwardly to give the fit shown in Fig. 16. The final refined structural coordinates are $a=8.8943(13)$ Å, $b=6.3805(8)$ Å, and $c=6.2002(10)$ Å with atoms at $(0,0.2314(5),\frac{1}{4})$ and (0.2647(4),0.0429(4),0), respectively. The *oI*16 structure is shown in Fig. 17 and it closely resembles that of fcc. Each atom in the structure has 12 nearest neighbors in the range of 2.9–3.5 Å, comprising four atoms with the same Wyckoff site symmetry and eight atoms with the other site symmetry.

Although the *Ibam* structure gives an excellent fit to the Pr-VII profile, close inspection of the observed and calculated profiles revealed a small (~0.06°) splitting of the (440) reflection at 18.3° that cannot be accounted for by the *Ibam* structure [see inset (a) of Fig. 16]. This suggests that the true structure of Pr-VII might have a lower symmetry than orthorhombic. Only the (440) reflection has any observable splitting even in the highest-resolution diffraction profiles (no such splitting was observed before annealing—see inset of Fig. 13), and there is thus too little information to determine

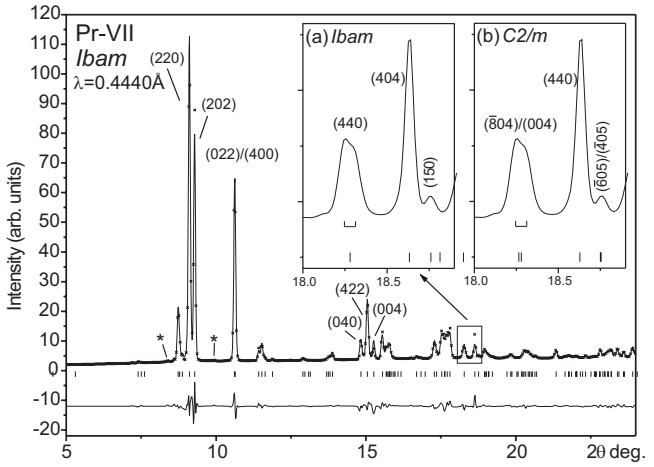

FIG. 16. Rietveld refinement of the orthorhombic *Ibam* structure to the diffraction pattern of Pr-VII obtained at 19.0 GPa. Indices are given for key reflections and asterisks mark contaminant peaks. The tick marks below the profile show the calculated peak positions, and the difference between the observed and calculated profiles is shown below the tick marks. The insets show enlarged views of the split peak at 18.3°, and the calculated peak positions in the best fitting (a) *Ibam* and (b) $C2/m$ Rietveld refinements. The horizontal bar immediately beneath the split peak in both insets shows the measured magnitude of the splitting—assuming the peak to be a doublet.

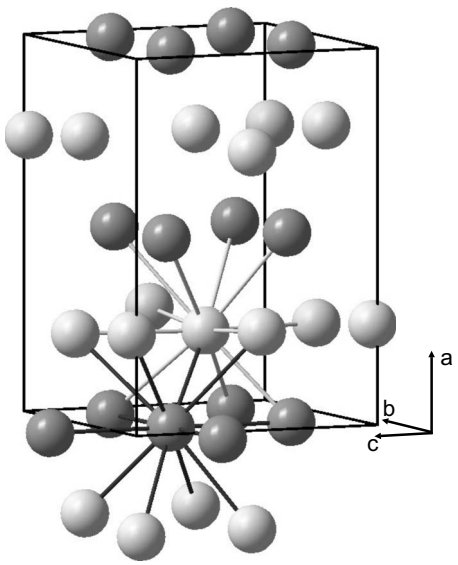

FIG. 17. The *Ibam* structure of Pr-VII. The atoms on the 8*g* and 8*i* sites are shown using light and dark atoms, respectively, and the bonds between different atoms identify the 12 nearest neighbors around each atom type.

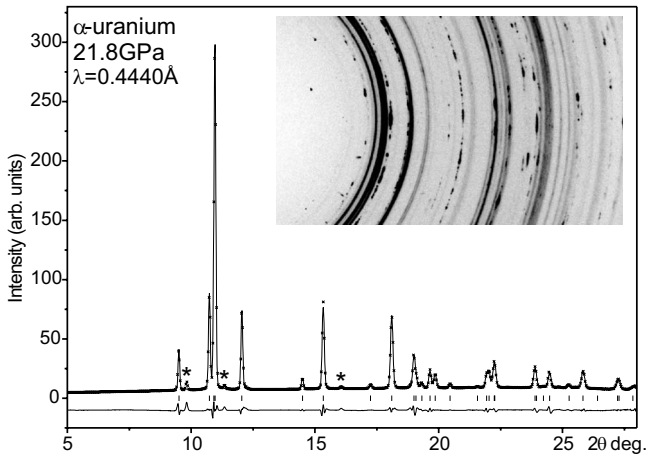

FIG. 18. Rietveld refinement of the *oC*4 structure to a diffraction profile from Pr at 21.8 GPa. The tick marks below the profile show the calculated peak positions, and the difference between the observed and calculated profiles is shown below the tick marks. Asterisks identify contaminant peaks. The inset shows part of a 2D diffraction image collected from a mixed-phase Pr-VII/ α-U sample at 20.0 GPa, illustrating the spotty nature of the Debye-Scherrer rings from the α-U phase.

whether the structure truly is distorted from orthorhombic, let alone determine the lattice type. We note that although the monoclinic *mC*16 structure proposed by Dmitriev *et al.* does predict this reflection to be a doublet [but only when $b<c$, as in the refinement shown in Fig. 14 and inset (b) of Fig. 16], the calculated splitting in our best-fitting refinement of this structure is a factor of more than 4 smaller than that actually observed [see inset (b) of Fig. 16].

G. Structure α-U Pr

The transition of Pr-VII to the collapsed α-U phase was observed at 20.5(5) GPa on pressure increase, and single-phase patterns were obtained above 21.5 GPa. A diffraction profile from this phase at 21.8 GPa is shown in Fig. 18. As reported previously,[24] the transition to the α-U phase is accompanied by recrystallization of the sample. This is illustrated in the inset of Fig. 18, which shows the "spotty" nature of the α-uranium diffraction peaks.

The structure of the α-U phase is orthorhombic, space group *Cmcm*, with atoms on the 4*c* site at $(0,y,\frac{1}{4})$. The Pearson symbol is therefore *oC*4. The lattice parameters at 21.8 GPa are $a=2.7743(1)$ Å, $b=5.6165(2)$ Å, and $c=4.8924(3)$ Å [volume/atom=19.06(1) Å^3], and the refined value of the atomic coordinate is 0.0972(2), somewhat smaller than the values in the two other elements in which this parameter has been determined—uranium 0.1023(2) (Ref. 1) and cerium 0.1014(2).[19]

IV. DISCUSSION

The measured compressibility of Pr to 23 GPa is shown in Fig. 19. In contrast to the studies of Chesnut and Vohra[20] and Dmitriev *et al.*,[22] both of which suggested a discontinuity in the compressibility of Pr as a result of the transition to Pr-VII, we observe no such change—our atomic volume data for Pr-VII in the range of 18–20 GPa lie on the extension of the compressibility curve established by the *hR*24 data. While the gradual disappearance of diffraction peaks from *hR*24 during the *hR*24 to Pr-VII transition suggests that it may be first order, the compressibility data suggest that any volume change at the transition will be very small. Also shown in Fig. 19 are the atomic volume data for Pr-VII obtained from Fig. 4 of Dmitriev *et al.*, which are in very poor agreement with the current data. However, as said previously, the compressibility data shown in that study are not in agreement with the (two different) atomic volumes given by the same authors for Pr-VII at 19.1 GPa. If these data are plotted (Fig. 19), then the agreement with the present results is excellent. The atomic volume given by Chesnut and Vohra[20] for the d-fcc phase at 15 GPa is also in very poor agreement with the present results. If, however, the corrected lattice parameters (see previous discussion) are used, then the agreement with the present work is, once again, excellent. In their determination of the structure of Pr-VII, Dmitriev *et al.*[22] reported that the change in compressibility at the d-fcc to Pr-VII transition, without any accompanying volume change, provided evidence of a structure having itinerant 4*f*

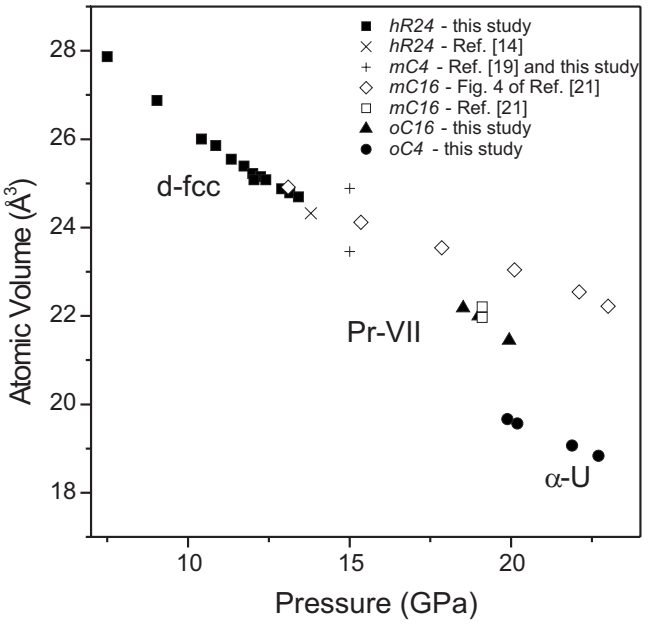

FIG. 19. The measured compressibility of Pr from 7 to 23 GPa. Data points from the present study are shown using filled squares, circles, and triangles for the d-fcc, Pr-VII, and α-U phases, respectively. The cross (×) shows the atomic volume of the *hR*24 structure at 13.8 GPa, as determined by Hamaya *et al.* (Ref. 15). The open diamonds show the data for Pr-VII from Fig. 4 of Dmitriev *et al.* (Ref. 22), while the two open squares mark the atomic volumes for Pr-VII obtained from the given lattice parameters of Pr-VII at 19.1 GPa (22.20 Å^3) (Ref. 22) and the atomic volume at the same pressure (21.969 Å^3) as given in the caption of Fig. 3 in Ref. 22. Also shown, using plus symbols (+), are the atomic volumes of the d-fcc phase at 15 GPa as calculated from the given lattice parameters in Ref. 20 (24.88 Å^3) and that obtained from the revised lattice parameters obtained from a reanalysis of the same data in this study (23.46 Å^3).

electrons but not being "precollapsed." The results of this study lead us to question this, as there is no evidence of a compressibility change, and therefore electronic change, at the d-fcc to Pr-VII transition. Insight into the reasons for the transition, such as a phonon instability,[22] might be obtained from *ab initio* calculations, and such calculations are planned for the future.

The redetermination of the structure of Pr-VII enables us to provide a new estimate for the volume change ($\Delta V/V_{trans}$) at the Pr-VII$\rightarrow\alpha$-uranium transition that arises as a result of electron delocalization. From a mixed-phase profile, the volume change is determined to be 8.3(1)%, smaller than the ~9.8% reported by Smith and Akella,[7] the ~9.5% reported by Grosshans,[8] the 9.1% reported by Cunningham *et al.*,[24] and the ~11% shown by Dmitriev *et al.*[22] Our value is also a factor of 2 smaller than the value 16.7% quoted by Chesnut and Vohra,[20] although in this case the different value results from a misindexing of the diffraction data.

We believe it is now possible to present a consistent description of the pressure dependence of Pr from 7 to 23 GPa. At 7.4 GPa, the fcc phase transforms into the d-fcc phase which is rhombohedral, with space group $R\bar{3}m$, and 24 atoms in the equivalent hexagonal cell (*hR*24). The fcc$\rightarrow$*hR*24 transition is first order, but there is no detectable discontinuity in the atomic volume, lattice parameters, or atomic coordinates at the transition. On further compression, the *hR*24 structure undergoes a transition to Pr-VII beginning near 13.7 GPa. This transition occurs over a wide pressure range, is probably first order, and single-phase patterns of Pr-VII are obtained only above 18 GPa. The structure of Pr-VII is body-centered orthorhombic with space group *Ibam* with 16 atoms per cell, or a very small distortion of this, which results in the observable splitting of a single high-angle diffraction peak. Pr-VII transforms to the orthorhombic α-uranium phase at 20.5(5) GPa, with an accompanying volume change of 8.3(1)%, and this is stable to 147(5) GPa, where it undergoes a transition to a primitive orthorhombic structure.[36]

Finally, the confirmation of a new phase in Pr between the previously well-known d-fcc and collapsed phases begs the question as to whether such a phase is unique to Pr or whether it might also be found in other lanthanides. To investigate this we have made preliminary studies of praseodymium's neighboring element, neodymium. Figure 20 shows a sequence of diffraction patterns from the d-fcc phase of Nd on pressure increase from 23.6 to 27.5 GPa. First we note that the weak reflections that distinguish the *hR*24 and *mC*4 descriptions of the d-fcc phase are clearly present in Nd and that the structure is thus definitely *hR*24. At 25.8 GPa there is clear evidence of changes in the diffraction pattern that are very similar to those found in Pr (compare the insets of Figs. 12 and 20). These changes do not arise from a transition to the α-U phase, which is observed only above 41 GPa in Nd.[37] Unfortunately, annealing the Nd sample at 27.5 GPa and 473 K for several hours did not result in a noticeable sharpening of the pattern, and further analysis and better samples will be required in order to show that this new phase does indeed have the same structure as Pr-VII. However, there is strong evidence to suggest that a previously unknown phase *is* observed in at least one other lanthanide between the d-fcc and α-U phases and that this might therefore be an additional member of the lanthanide structural sequence.

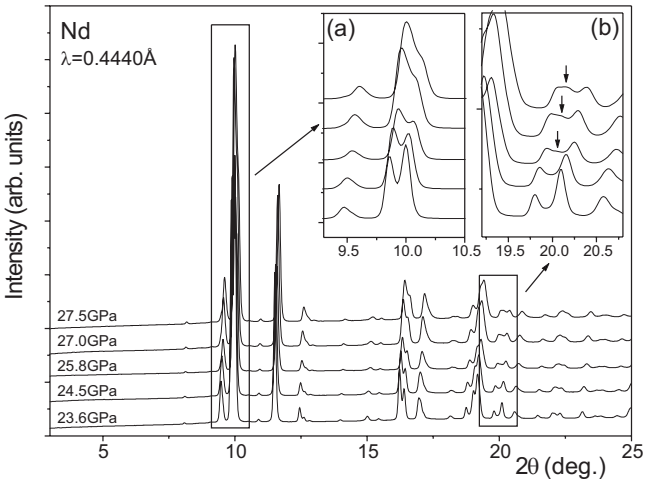

FIG. 20. Diffraction profiles obtained from *hR*24-Nd on pressure increase from 23.6 to 27.5 GPa. The insets show how (a) the (006)/(202) and (b) the (00,12)/(404) doublets (as indexed on the *hR*24 structure) evolve on pressure increase. The new reflection that appears between the (00,12) and (404) peaks is indicated with an arrow in inset (b).

ACKNOWLEDGMENTS

We thank A. Lennie of Daresbury Laboratory for setting up the 9.5HPT beamline and M. Hanfland and M. Roberts of the ESRF and Daresbury Laboratory, respectively, for assistance in setting up beamlines ID09 and 9.1. We express our gratitude to U. Schwarz of the MPI für Chemische Physik fester Stoffe for providing the high-purity samples of Pr and Nd. This work was supported by grants and a studentship from EPSRC, funding from CCLRC and STFC, and facilities provided by Daresbury Laboratory and the ESRF.

[1] J. Donohue, *The Structure of the Elements* (Robert E. Krieger, Malabar, FL, 1982).

[2] W. A. Grosshans and W. B. Holzapfel, Phys. Rev. B **45**, 5171 (1992).

[3] U. Benedict, J. R. Peterson, R. G. Haire, and C. Dufour, J. Phys. F: Met. Phys. **14**, L43 (1984).

[4] H. K. Mao, R. M. Hazen, P. M. Bell, and J. Wittig, J. Appl. Phys. **52**, 4572 (1981).

[5] P. Villars and L. D. Calvert, *Pearson's Handbook of Crystallographic Data for Intermetallic Phases*, 2nd ed. (Am Soc Micro-

biol, Materials Park, OH, 1991).
[6] In trying to review the extensive background literature on Pr, confusion can arise due to the different nomenclatures used by different authors. To help the reader distinguish the various high-pressure phases from the crystal structures of those phases, we use terms such as fcc, d-fcc, Pr-VII, and α-U for the former and Pearson notation ($oP16$, $hR24$, etc.) to denote the latter.
[7] G. S. Smith and J. Akella, J. Appl. Phys. **53**, 9212 (1982).
[8] W. A. Grosshans, Y. K. Vohra, and W. B. Holzapfel, J. Phys. F: Met. Phys. **13**, L147 (1983).
[9] G. S. Smith and J. Akella, Phys. Lett. **105A**, 132 (1984).
[10] W. A. Grosshans, Y. K. Vohra, and W. B. Holzapfel, Phys. Rev. Lett. **49**, 1572 (1982).
[11] Y. K. Vohra, V. Vijayakumar, B. K. Godwal, and S. K. Sikka, Phys. Rev. B **30**, 6205 (1984).
[12] T. Krüger, B. Merkau, W. A. Grosshans, and W. B. Holzapfel, High Press. Res. **2**, 193 (1990).
[13] R. G. Haire, S. Heathman, and U. Benedict, High Press. Res. **2**, 273 (1990).
[14] O. Shimomura, K. Takemura, H. Fujihisa, Y. Fujii, Y. Ohishi, T. Kikegawa, Y. Amemiya, and T. Matsushita, Rev. Sci. Instrum. **63**, 967 (1992).
[15] N. Hamaya, Y. Sakamoto, H. Fujihisa, Y. Fujii, K. Takemura, T. Kikegawa, and O. Shimomura, J. Phys.: Condens. Matter **5**, L369 (1993).
[16] N. Hamaya, N. Okabe, M. Yamakata, T. Kagi, and O. Shimomura, High Press. Res. **14**, 287 (1996).
[17] F. Porsch and W. B. Holzapfel, Phys. Rev. B **50**, 16212 (1994).
[18] K. Syassen, A. Grzechnik, J. Köhler, and I. Loa, ESRF Experimental Report No. HS1132 (2000) (unpublished).
[19] M. I. McMahon and R. J. Nelmes, Phys. Rev. Lett. **78**, 3884 (1997).
[20] G. N. Chesnut and Y. K. Vohra, Phys. Rev. B **62**, 2965 (2000).
[21] B. J. Baer, H. Cynn, V. Iota, C.-S. Yoo, and G. Shen, Phys. Rev. B **67**, 134115 (2003).
[22] V. P. Dmitriev, A. Yu. Kuznetsov, O. Bandilet, P. Bouvier, L. Dubrovinsky, D. Machon, and H.-P. Weber, Phys. Rev. B **70**, 014104 (2004).
[23] H. Olijnyk, W. A. Grosshans, and A. P. Jephcoat, Phys. Rev. Lett. **93**, 255505 (2004).
[24] N. C. Cunningham, N. Velisavljevic, and Y. K. Vohra, Phys. Rev. B **71**, 012108 (2005).
[25] G. J. Piermarini, S. Block, and J. D. Barnett, J. Appl. Phys. **44**, 5377 (1973).
[26] H. K. Mao, J. Xu, and P. M. Bell, J. Geophys. Res. **91**, 4673 (1986).
[27] A. P. Hammersley, S. O. Svensson, M. Hanfland, A. N. Fitch, and D. Hausermann, High Press. Res. **14**, 235 (1996).
[28] V. Petricek and M. Dusek, *The Crystallographic Computing System JANA2000* (Institute of Physics, Praha, 2000).
[29] J. W. Otto, J. K. Vassiliou, and G. Frommeyer, Phys. Rev. B **57**, 3253 (1998).
[30] R. J. Angel, M. Bujak, J. Zhao, G. D. Gatta, and S. D. Jacobsen, J. Appl. Crystallogr. **40**, 26 (2007).
[31] A. K. Singh, C. Balasingh, H. K. Mao, R. J. Hemley, and Jinfu Shu, J. Appl. Phys. **83**, 7567 (1998).
[32] T. Kenichi and A. K. Singh, Phys. Rev. B **73**, 224119 (2006).
[33] J. M. Leger, N. Yacoubi, and J. Loriers, Mater. Res. Bull. **14**, 1431 (1979).
[34] S. Kern, C.-K. Loong, J. Faber, and G. H. Lander, Solid State Commun. **49**, 295 (1984).
[35] W. L. Korst and J. C. Warf, Inorg. Chem. **5**, 1719 (1966).
[36] N. Velisavljevic and Y. K. Vohra, High Press. Res. **24**, 295 (2004).
[37] W. A. Grosshans and W. B. Holzapfel, J. Phys. (Paris), Colloq. **45**, C8 (1984).